Fish aggregating devices drift like oceanographic drifters in the near-surface currents of the Atlantic and Indian Oceans

T. Imzilen[a], E. Chassot[a,b], J. Barde[c], H. Demarcq[a], A. Maufroy[a,d], L. Roa-Pascuali[a], J-F. Ternon[a], C. Lett[e,*]

[a]*MARBEC, IRD, Ifremer, Univ Montpellier, CNRS, Sète, France*
[b]*Seychelles Fishing Authority, PO BOX 449, Victoria, Seychelles*
[c]*Institut de Recherche pour le Développement (IRD), Indian Ocean Commission, Ébène, Mauritius*
[d]*ORTHONGEL, 11 bis rue des sardiniers, 29 900 Concarneau, France*
[e]*IRD, Sorbonne Université, Unité de Modélisation Mathématiques et Informatique des Systèmes Complexes, UMMISCO, F-93143, Bondy, France*

Abstract

Knowledge of ocean surface dynamics is crucial for oceanographic and climate research. The satellite-tracked movements of hundreds of drifters deployed by research and voluntary observing vessels provide high-frequency and high-resolution information on near-surface currents around the globe. Consequently, they constitute a major component of the Global Ocean Observing System (GOOS). However, maintaining this array is costly and in some oceanic regions such as the tropics, spatio-temporal coverage is limited. Here, we demonstrate that the GPS-buoy equipped fish aggregating devices (FADs) used in tropical tuna fisheries to increase fish catchability are also capable of providing comparable near-surface current information. We analyzed millions of position data collected between 2008 and 2014 from more than 15,000 FADs and 2,000 drifters, and combined this information with remotely-sensed near-surface current data to demonstrate that the surface velocity components of FADs and drifters are highly correlated in the Atlantic and Indian Oceans. While it was noted that the subsurface structures of FADs (typically made of recycled fishing nets) did slow them down

*Corresponding author
Email address: `christophe.lett@ird.fr` (C. Lett)

relative to the drifters, particularly in the Atlantic Ocean, this bias was measurable and could be accounted for in future studies. Our findings show that the physical meteorological and oceanographic data collected by fishermen could provide an invaluable source of information to the GOOS. Furthermore, by forging closer collaborations with the fishing industry and ensuring their contributions to global ocean databases are properly acknowledged, there is significant scope to capture this data more effectively.

Keywords: drifter, fisheries, Lagrangian transport, oceanography, surface currents

Introduction

Oceans cover 70% of the Earth's surface and are much harder to observe than terrestrial systems (Richardson and Poloczanska, 2008). For centuries, mariners have been observing the states of oceans and the atmosphere by recording oceanographic and physical meteorological data near the ocean's surface (Woodruff et al., 1987). As early as the nineteenth century, international collaborative efforts were initiated to coordinate the collection and curation of ocean-atmosphere data from voluntary observing ships (VOS) and build large-scale marine data sets. Such data sets are now considered essential for oceanographic and climate studies (Woodruff et al., 1987; Kent et al., 2010; Freeman et al., 2017). From the 1970s, ocean data collection was revolutionized with the advent of satellite technology and the development of sensors that were capable of measuring a large range of oceanographic and atmospheric features (Martin, 2004).

Combining *in-situ* and remotely-sensed satellite observations has proven to be an essential step to improving our understanding of how ocean circulation affects climate at regional and global scales through the transport of water and heat received from the sun (Maximenko et al., 2009; Lee et al., 2010). Remotely-sensed measurements of sea surface temperature, altimetry and vector winds provide a synoptic view of ocean surface current patterns at consistent and regular spatial and temporal scales (Lagerloef et al., 1999; Sudre and Morrow, 2008; Dohan and Maximenko, 2010). At a finer scale, *in-situ* velocity measurements of near-surface currents are routinely collected by satellite-tracked drifters maintained by the Global Drifter Program (GDP), an operational component of the Global Ocean Observing System (GOOS) and the Global Climate Observing System (GCOS). This data provides a direct measurement of water properties and complements the satellite data by supplying information on high-frequency, small-scale oceanic processes (Niiler and Paduan, 1995; Reverdin et al., 2003; Lumpkin and Elipot, 2010). These drifters are floating devices that comprise a surface buoy equipped with a satellite transmitter and a subsurface sea anchor (Fig. 1). Since the 2010s, the GDP has maintained a global array of ∼1,200-1,500 drifters that have been deployed from VOS, research vessels and planes to cover the world's oceans (Joseph, 2013; Lumpkin and Johnson, 2013; Elipot et al., 2016). In addition to supporting oceanographic and climate research, the ocean circulation information acquired by these systems has been instrumental in supporting both military and civil applications, including search and rescue operations that use the data to improve their field of search predictions (Davidson et al., 2009). More recently, their role in tracking floating debris (Law et al., 2010; Cózar et al., 2014) has garnered attention as concerns about marine plastics pollution increase.

A knowledge of ocean dynamics is also key for fishermen who use it to both navigate and find fish resources. Monitoring surface water characteristics is essential in pelagic fisheries where the use of satellite remote-sensing has long been recognized as a fish harvesting aid (Simpson, 1992; Chassot et al., 2011). Modern fishing vessels are now equipped with a large range of sensors and electronic tools that constantly monitor the marine environment, enabling fishermen to identify the suitable habitats of target fish species (e.g. Torres-Irineo et al., 2014). In tuna fisheries, the purse seine vessels that target fish schools have extensively deployed satellite-tracked fish aggregating devices (FADs) over the last decade. Typically made of a bamboo raft equipped with floats (to ensure buoyancy) and a sea anchor built of old fishing nets (Fig. 1), these FADs attract tuna and increase fishery productivity (Fonteneau et al., 2013; Maufroy et al., 2017). In recent years, the number of GPS-buoy equipped FADs used globally in this fishery has increased markedly. Currently, it is estimated that more than 100,000 FADs are now drifting around the globe at any given time (Baske et al., 2012; Scott and Lopez, 2014). While the average lifespan of a FAD at sea is shorter than a typical drifter, there are many more in circulation, particularly in the tropical areas where the purse seine fleets operate. Consequently, it is likely that FADs could provide the GDP with complementary data, particularly in equatorial regions. Given that these areas are currently under sampled due to factors such as infrequent deployment of drifters and equatorial divergence (Lumpkin and Pazos, 2007), this increased FAD data coverage is especially important. As an illustrative case, a few FAD positions were used to complement the drifter data and ocean model outputs analyzed to locate the wreckage of the Air France flight that crashed in 2009 en route from Rio de Janeiro to Paris (Drévillon et al., 2013).

The overarching objective of this study is to test the hypothesis that FADs deployed by fishermen follow near-surface currents in the Atlantic and Indian Oceans. If true, this would mean that FAD data could provide valuable information on oceanic circulation. To test this hypothesis, we combined and analyzed large data sets from GDP drifters, a satellite-derived surface current product available from the Ocean Surface Currents Analyses Real-time (OSCAR) processing system and approximately 5 million FAD positions collected by French tuna fishing companies between 2008 and 2014. To begin with, we directly compared the velocities of FAD and drifter pairs observed in close proximity over similar time periods. We then used the OSCAR currents as an indirect comparison point for both the FAD and drifter data. For the large biogeographical provinces of the Atlantic and Indian Oceans (Longhurst, 2007), we estimated the correlations between the OSCAR currents and the observed FAD and drifter velocities. We then compared FAD and drifter movements with short-term OSCAR current projections.

Material ans methods

Fish Aggregating Devices

The GPS locations of the buoys attached to the FADs used by the French fishing fleet operating in the Atlantic and Indian Oceans have been available since 2008 through a collaborative agreement between the Institut de Recherche pour le Développement (IRD) and the French frozen tuna producers' organization ORTHONGEL. The full methodology used to filter and process the raw GPS data to derive FAD trajectories at sea can be found in Maufroy et al. (2015). The current FAD data set consists of 4,777,524 positions, belonging to a total of 21,047 distinct buoys that were deployed at sea between 2008 and 2014. The periodicity of FAD position varies from 15 minutes (minimum) to 2 days (maximum). This function can be remotely modified to facilitate detection when a vessel is on its final approach to a

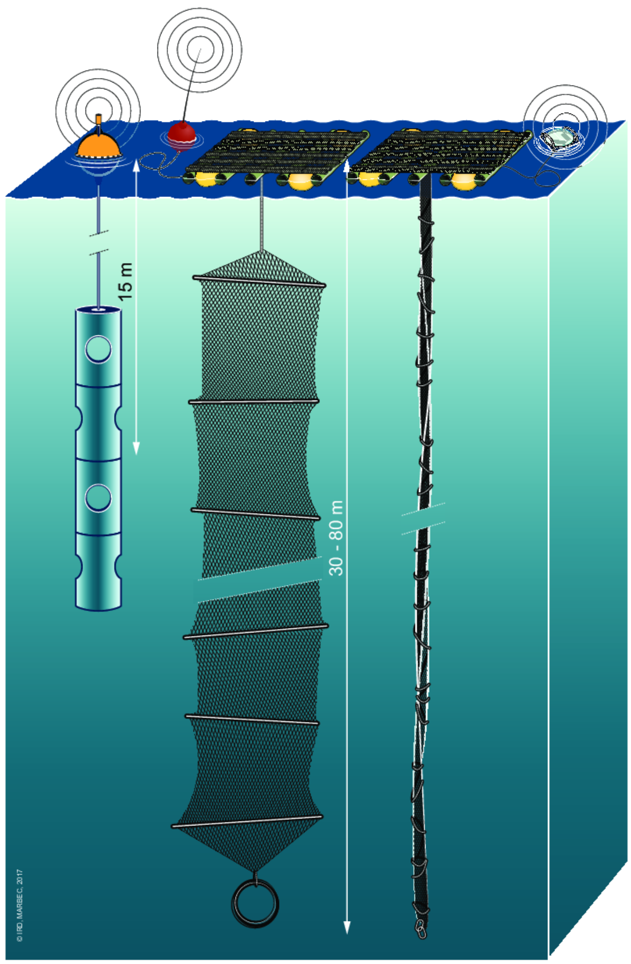

Figure 1: Description of the structure and design (in the water column) of a typical drifter (left), fish aggregating devices (FADs) used in purse seine fisheries with a sea anchor made of 'curtain' nets (middle), and 'sausage' nets (right).

FAD. Approximately 20% of the FAD data set consists of contiguous locations emitted within a time period of less than 6 hours and most FADs emitted two contiguous signals within a 24-hour period. FADs generally consist of bamboo rafts covered in old pieces of purse seine nets with several floats that ensure their buoyancy (Fig. 1). The subsurface structures found below FADs are typically made out of old fishing nets and extend to depths of 30-80 m (Franco et al., 2009). Initially, these nets hung in 'curtains', but newer designs feature 'sausages' of nets or ropes. This design was introduced to prevent the entanglement of fish and turtles. French GPS buoys have also been deployed on floating objects of natural (e.g. palm trees, logs) or anthropogenic (e.g. ropes) origins that represented about 20% of all floating objects encountered at sea by observers on French purse seiners during 2008-2014, with the Mozambique Channel being characterized by a relatively high percentage of these natural objects (Maufroy et al., 2017).

Surface drifters

The drifters are made up of a surface buoy (∼30 cm diameter) that is attached by a long, thin tether to a holey sock drogue (sea anchor) that is centered at ∼15 m below the surface (Fig. 1). The buoy measures sea surface temperature and other properties such as air pressure and wind direction and sends this information to passing satellites using an ARGOS transmitter (Lumpkin and Pazos, 2007). While the size of the buoy and drogue can vary, their drag area ratio is standardized, which acts to constrain their downwind slip (Niiler and Paduan, 1995). The GDP archives most of the data collected by the drifters. We downloaded our data set (1,092,362 positions belonging to 2,285 distinct, drogued drifters having occurred in the Indian and Atlantic Oceans during 2008-2014) from `ftp://ftp.aoml.noaa.gov/phod/pub/buoydata/`. Hansen and Poulain (1996) detail the corrections that are applied to the raw data.

Data filtering

A very small number of velocity values collated from the IRD and GDP databases were found to be inconsistent with the maximum speed expected for ocean currents. We therefore removed data points that had velocity values higher than the 99.99% quantile values of 471.6 cm s^{-1} (i.e. 9.17 knots) and 234 cm s^{-1} (i.e. 4.55 knots) for fish aggregating devices (FADs) and drifters, respectively.

Data distribution

There is twice as much data for the Indian Ocean as the Atlantic Ocean but overall, the number of FAD locations has increased markedly in both oceans over the study period while the amount of drifter data remained relatively constant (Table 1). This reflects the significant expansion in the FAD fishery that has taken place in both regions (Maufroy et al., 2017). In this study, we focused on eight large biogeographical provinces, four of which occurred in the Atlantic Ocean (i.e. Guinea Current Coastal (GUIN), Eastern Tropical (ETRA), North Atlantic Tropical (NATR), and Western Tropical Atlantic (WTRA)) and four of which occurred in the Indian Ocean (East Africa Coastal (EAFR), North West Arabian Upwelling (ARAB), Indian Monsoon Gyres (MONS), and Indian Southern Subtropical Gyre (ISSG)) (Longhurst, 2007). The total number of FAD data points collated for these provinces was >50,000 (Appendix Table A1).

Table 1: Annual number of fish aggregating device (FAD) and drifter observations analyzed in the Atlantic and Indian Ocean.

Device	ocean	2008	2009	2010	2011	2012	2013	2014
FADs	Atlantic	17,849	45,469	102,216	153,990	286,156	322,490	464,930
FADs	Indian	105,356	149,211	200,983	382,315	580,547	784,130	1,181,882
Drifters	Atlantic	93,540	108,828	84,912	65,851	75,974	118,125	87,067
Drifters	Indian	51,479	38,311	48,303	46,603	52,377	80,777	140,215

Satellite currents

The satellite-derived surface current information produced by the OSCAR processing system is provided in near-real time from a combination of quasi-steady geostrophic and locally wind-driven dynamics (Lagerloef et al., 1999) (`http://www.oscar.noaa.gov`). The OSCAR product combines: (i) a geostrophic term computed from the gradient of ocean surface topography fields using several sources of spatial observation through time, (ii) a wind-driven velocity term computed from an Ekman-Stommel formulation with variable eddy viscosity using QuikSCAT and National Centers for Environmental Prediction winds, and (iii) a thermal wind adjustment using Reynolds sea surface temperature (Reynolds and Rayner, 2002). Dohan and

Maximenko (2010) provide a full description of the OSCAR product. In this study, we used the 1/3 degree grid and 5-day interval resolution of the OSCAR currents, which is designed to represent a 30 m surface layer average. The OSCAR currents have been validated with moored buoys, drifters, and shipboard acoustic Doppler current profilers (Johnson et al., 2007).

Direct comparison

To compare possible velocity differences between the floating devices, we selected every FAD and drifter pair that emitted a signal in near space and time. Thus, for each FAD location and 24-hour time period, we searched for a drifter within a 1/6 degree radius (∼10 nm). If several drifters were identified, we selected the device that was closest in time. A sensitivity analysis, with time periods of 12 hours and 2.5 days (consistent with the OSCAR temporal resolution), was then conducted. The correlation between the corresponding zonal and meridional velocity components for the FAD and drifter pairs was then considered using the Pearson's correlation coefficient (Johnson et al., 2007). We then used major axis regression models (forced through the origin) to assess the agreement between the two variables (Legendre and Legendre, 1998; Warton et al., 2006). This approach accounts for the measurement errors in both variables.

Indirect comparison

This comparative analysis was then extended to the full data set by undertaking an indirect comparison of FAD and drifter velocities using satellite measurements of near-surface current velocities. At each FAD and drifter position, we linearly interpolated the OSCAR current data in time and space to calculate the OSCAR velocities (Johnson et al., 2007; Dohan and Maximenko, 2010). To determine the correlation and agreement between the FADs and OSCAR and drifters and OSCAR, we used the methodology described in the previous section. This analysis was completed at both the basin and large biogeographical province (Longhurst, 2007) scales to ensure that the different oceanographic regimes of the Indian and Atlantic Oceans were represented. The spatio-temporal autocorrelation of velocity values along the FAD and drifter trajectories was accounted for by subsampling the data at values that were close (5 days) and far above (15 days) the Lagrangian integral time scale estimated for drifters in the Indian Ocean (i.e. 2-7 days; Peng et al., 2014).

Projection of FAD and drifter locations using OSCAR

The OSCAR velocities were then used to project the FAD and drifter locations from one timestep to the next to compare their Lagrangian transport in near-surface waters. We computed the distance d between the projected location and the next observed location and the distance D between the current location and next observed location to estimate the index d/D for FADs and drifters. These indices were used to gauge the degree of departure of each floating device from the OSCAR currents predictions (Berta et al., 2014; Yaremchuk et al., 2016). Index values that were larger than the 99% quantile values observed in the data sets were removed and then their distributions were compared (i.e., for FADs and drifters) at both the basin and (selected) large biogeographical province scales.

Results

At the basin scale, the velocity distributions of FADs and drifters were different. In the Atlantic Ocean, the first quartile, median, and third quartile values in the FAD and drifter velocity distributions were 11.45, 19.96, 32.8 cm s^{-1}, and 9.15, 15.11, 24.36 cm s^{-1}, respectively. The velocities of both device types were found to be higher in the Indian Ocean where these values were 21.58, 35.13, 54 cm s^{-1} for FADs and 14.78, 24.5, 38.44 cm s^{-1} for drifters. At a regional scale, FAD and drifter velocities were similar in the ETRA, NATR, and WTRA biogeographical provinces of the inter-tropical Atlantic Ocean, but they differed in the GUIN province (Appendix Table A2). In that province, the number of drifter locations was the lowest, more than an order of magnitude lower than the number of FAD locations (Appendix Table A1). Within the four provinces that make up most of the south-western Indian Ocean, FAD velocities were substantially higher than drifter velocities (Appendix Table A2). Differences in velocities between FADs and drifters were attributed to differences in the spatio-temporal distribution between the two types of devices. In the Atlantic Ocean, the FAD data were concentrated in the central-eastern region (Fig. 2A) while the drifter data were more evenly distributed, although the northern area showed the highest concentrations (Fig. 2B). In the Indian Ocean, the FAD data were concentrated in the central-western region (Fig. 2A) while the drifter data were more evenly distributed over the entire basin (Fig. 2B). At a smaller, 1° × 1° spatial scale, the FADs and drifters showed very similar patterns of velocity in the near-surface currents (Fig. 2C and D), revealing the major oceanographic features of both the tropical Atlantic Ocean (the South Equatorial and the North Brazil currents, the Equatorial countercurrent and the Guinea current) and the Indian Ocean (Somali, North Madagascar, and Agulhas currents, the Equatorial countercurrent and the South Equatorial current).

More than 18,000 pairs of FADs and drifters were detected across the Atlantic (n = 4,146) and Indian (n = 14,556) Oceans (Fig. 3). For these pairs, the zonal and meridional components of the FAD vs. drifter velocities were found to be significantly and highly correlated with Pearson's correlation coefficients between 0.68 and 0.93 (Fig. 4). This result was found to be robust to the time period considered for the definition of pairs of floating devices (Appendix Table A3). We also found several pairs in both oceans that shared common trajectories over several weeks to months, e.g., two FADs deployed in the Indian Ocean in 2013 traveled with two drifters during several months (Appendix Fig. A1). In the Indian Ocean, the velocity of FAD and drifter pairs agreed remarkably well (Fig. 4 and Appendix Table A3). In the Atlantic Ocean, however, small but consistent systematic differences in the velocity components indicate that drifters move faster than FADs (2-37% higher velocity components, 10-21% higher overall velocity; Fig. 4 and Appendix Table A3).

The outcomes of the comparative analysis of FAD and drifter velocities with OSCAR satellite current products further supports the case for using FADs for monitoring ocean surface dynamics. Here, the regional spatial patterns in both FAD and drifter velocities were consistent with the remotely-sensed surface currents. The ocean currents inferred from the FAD and drifter movement data for near-surface waters in both oceans were correlated in the same way, and to the same extent, with the satellite currents in the large biogeographical provinces. The correlation coefficients of velocity components between FADs and OSCAR and drifters and OSCAR were generally very similar (Fig. 5, Appendix Figs. A2-A5 and Appendix Table A4). After accounting for autocorrelation in the data, these relationships were still highly significant (Appendix Table A5). However, the OSCAR currents appeared to be slower than the currents derived from the *in-situ* data collected from

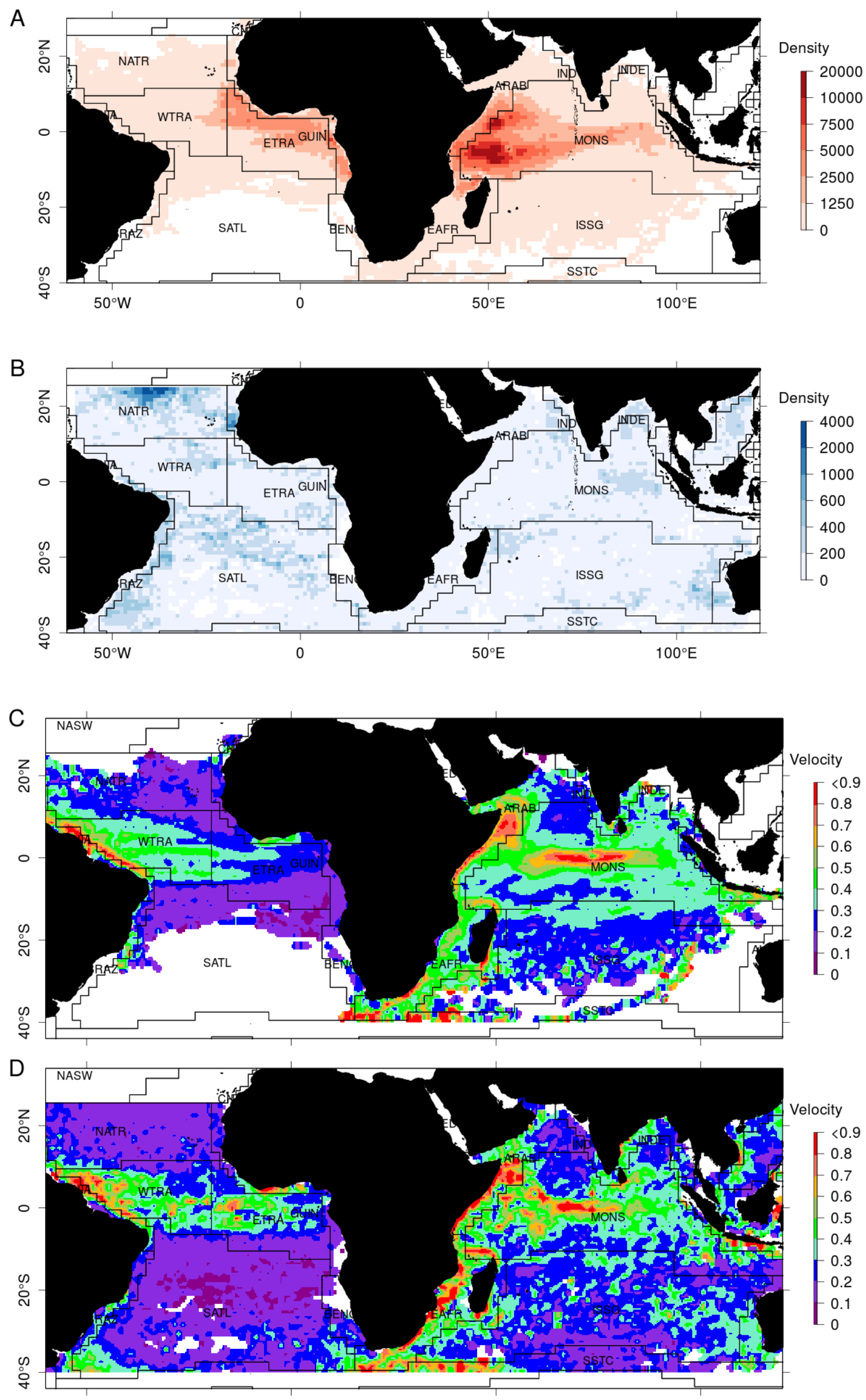

Figure 2: Spatial distribution of fish aggregating devices (FADs; A) and drifters (B) in the Atlantic and Indian Oceans within the defined geographical limits 60°W, 100°E longitude and 40°S, 30°N latitude. Density corresponds to the number of location points observed in each 1° × 1° grid cell for the time period 2008-2014. Mean of near-surface ocean currents (m s^{-1}) for the period 2008-2014, derived from FAD (C) and drifter (D) movements. Solid lines indicate boundaries between biogeographical provinces (Longhurst, 2007) (see Appendix Table A1 for acronyms).

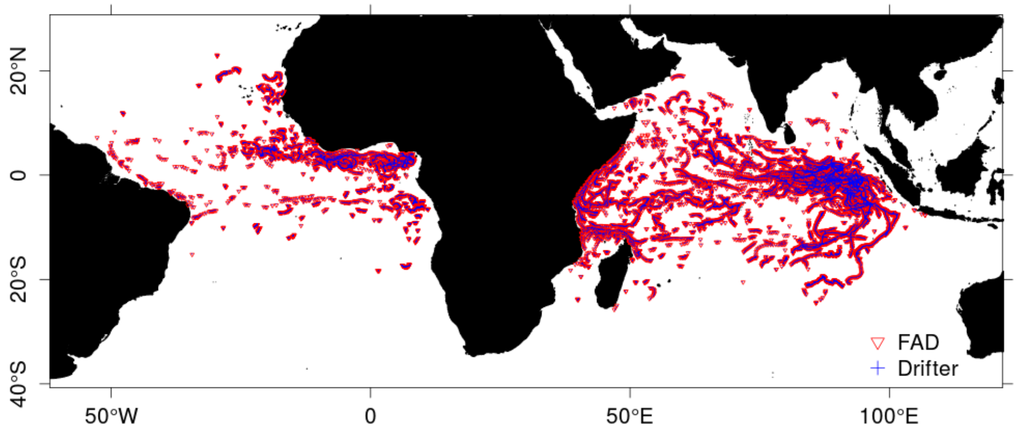

Figure 3: Spatial distribution of FADs (red triangles) and drifters (blue crosses) pairs that occurred within a 10 nm radius during 24-hour periods in the Atlantic (n = 4,146) and Indian (n = 14,556) Oceans.

the floating devices, as indicated by the slopes of the relationships between the OSCAR currents and floating devices being lower than 1 in all cases but one (Appendix Fig. A6 and Appendix Table A4). At the biogeographical province scale, the large variability observed in these slopes (FADs: 0.2-0.9 and drifters: 0.4-1.2) shows that they are not representing the surface dynamics at the same spatio-temporal scale.

The distributions of the OSCAR-projection error index d/D for FADs and drifters were almost identical across all biogeographical provinces (Appendix Fig. A7), with the notable exception in the south subtropical gyre province of the Indian Ocean (ISSG). Differences in spatial coverage explain this result, with FADs mostly occurring in the North of the ISSG province during the 2008-2014 period while drifters spanned the whole area (Fig. 2).

Discussion

We combined large data sets of remotely-sensed current speed with the GPS positions of thousands of satellite-tracked floating devices to show that the fish aggregating devices used in tuna fisheries and oceanographic drifters

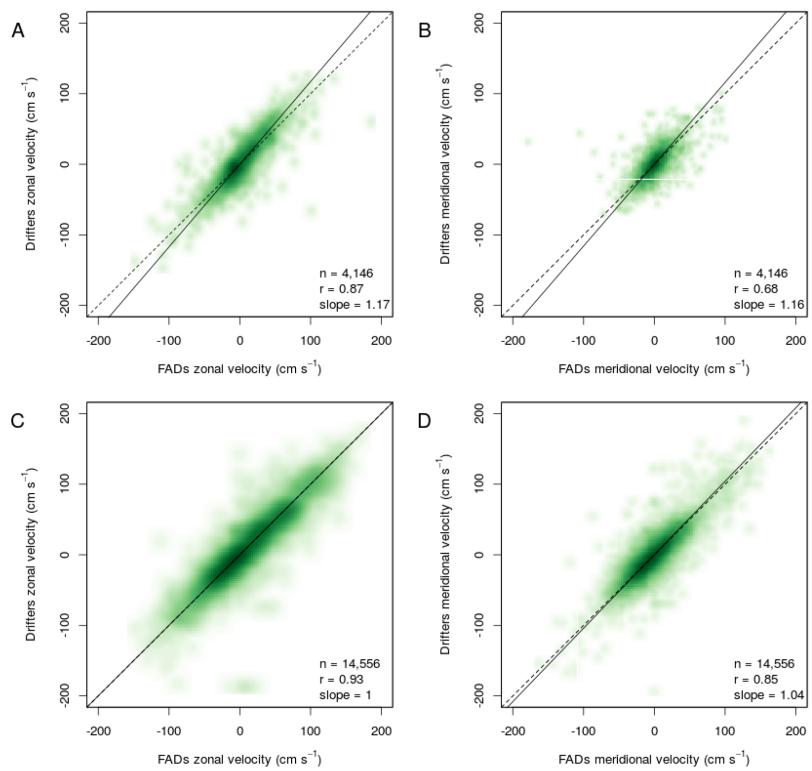

Figure 4: Velocity comparisons between the FAD and drifter pairs (A) zonal component in the Atlantic Ocean; (B) meridional component in the Atlantic Ocean; (C) zonal component in the Indian Ocean; and (D) meridional component in the Indian Ocean. The solid line indicates the major axis regression model and the dashed line indicates the 1:1 isoline.

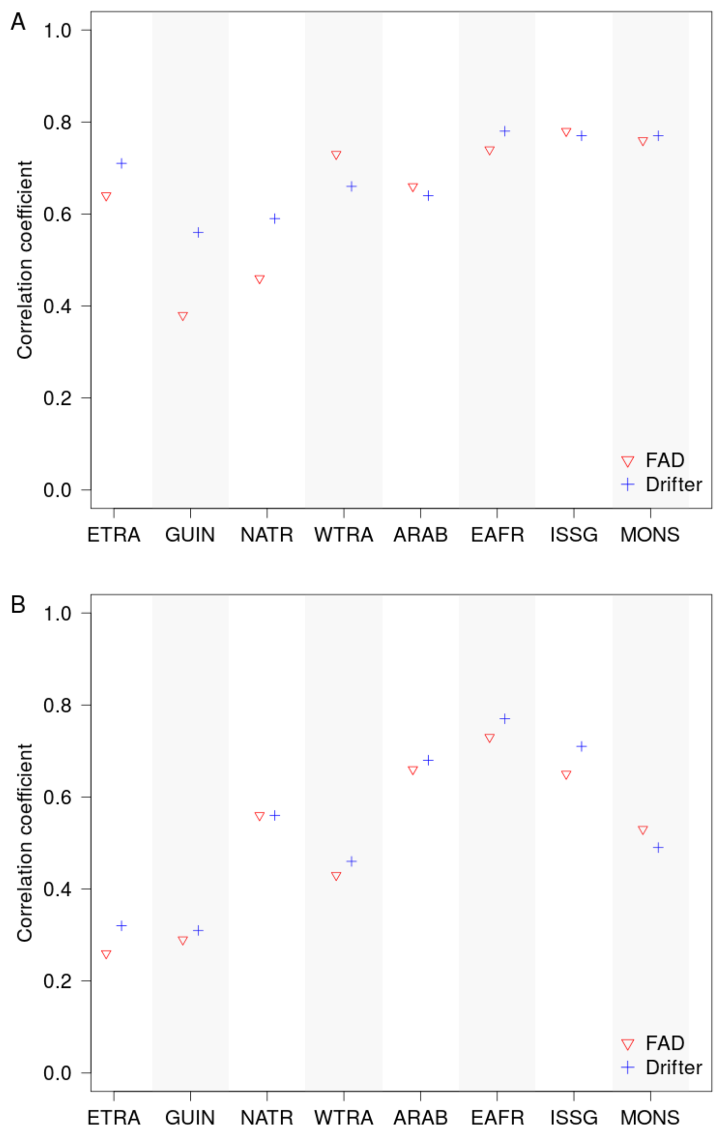

Figure 5: The comparison of correlation coefficients for the (A) zonal and (B) meridional components of velocity for the Ocean Surface Currents Analyses Real-time (OSCAR) versus fish aggregating devices (FADs) and OSCAR versus drifters in the selected Longhurst biogeographical provinces (see Appendix Table A1 for acronyms of the provinces and Fig. 2 for their location).

move similarly in near-surface ocean currents. This confirms that in tropical areas, the oceanographic information acquired by tuna fishermen could complement that gathered by the Global Ocean Observing System's drifter program. However, we highlighted some differences in the behaviour of FADs and drifters.

While drifters are anchored at around 15 m below the surface, the FADs subsurface structure composed of curtain or sausage nets can go down to 50-60 m in the Indian Ocean, 80 m in the Atlantic Ocean. These differences in anchoring depth between the two types of floating devices, and between FADs, locate them in different current layers. Indeed, we noted some speed differences between the two types of floating devices, particularly in the Atlantic Ocean, which are likely related to differences in their drogue structures. In the absence of strong winds, the geostrophic balance dominates the upper ocean circulation. In this case, floating devices with different windage and drogues at different depths, or even without drogue, move at similar velocities. Conversely, higher and variable winds generate internal waves as well as Ekman currents. The former modify the mixed layer depth whereas the latter generate currents that quickly rotate with depth. In both cases, floating devices with different drogue lengths will move with different velocities and often in different directions (Poulain et al., 2009). At smaller scales, non-linear dynamics arising from wind-vorticity generate convergence and divergence regions where floating devices drogued at various depth will respond in different ways.

In the Indian Ocean, velocities in the Equatorial countercurrent where many FADs occur have however been found to be relatively homogeneous along a 0-60 m depth range (Gnanaseelan and Deshpande, 2017), showing the same reversal pattern during monsoon periods. Depth homogeneous velocities were also reported along two modelled transects North of Madagascar and off Tanzania (Manyilizu et al., 2016), within two areas of high FAD occurrence. These conditions likely explain why velocities of drifter and FAD pairs compare so well in the Indian Ocean, despite differences in their design. By contrast, the eastern equatorial Atlantic Ocean is characterised by the prominence of the Equatorial Undercurrent (EUC), a strong permanent eastward flow located just below the westward South Equatorial current (Johns et al., 2014). FADs built and deployed in the Atlantic Ocean have tails going down to 80 m, longer than in the other oceans (Franco et al., 2009), and at a depth where the core of the EUC is found along the equator (Johns et al., 2014). These deep tails likely slow down the drift of the FADs as compared to the shallow subsurface structure of the drifters, explaining our results.

More generally and although the mechanisms of associative behavior of tuna to FADs remain poorly understood (Fréon and Dagorn, 2000), tuna fishermen consider that deeper tails increase the attraction of tunas by slowing down the FADs (Franco et al., 2009). Consequently, the depth of FAD appendages has been increasing in recent years in all oceans (Murua et al., 2018). In the eastern Pacific Ocean for instance, data collected by observers showed a substantial deepening of the net webbing from a median depth <10 m in the early 1990s to about 30 m nowadays (Hall and Roman, 2017). However, the progressive adoption of sausage nets and ropes in place of curtain nets, aimed at reducing the entanglement of marine species, may incidentally decrease the anchoring effect of the FAD tail appendage. In this study, our data came from fishing companies that use very similar FAD designs made of bamboo rafts and recycled fishing nets of similar lengths. More broadly, information on the structural design of FADs and their components is now being systematically collected through the fisheries observer programs run in both oceans. This new information will be useful to determine the influence of the subsurface currents on FAD drift. A comparison of the dispersion and separation of concurrently deployed drifter and FAD clusters would also provide insight into the extent to which design explains the observed differences in speed between the two types of floating devices.

Given that the FAD data we used in this study is open access, we expect that further analysis will be undertaken to fully validate the potential applications of FAD data for oceanographers, and that the results of this work will prompt long-term collaborations with the tuna fishing industry. The quantity of information available to the scientific community would strongly benefit from the release of data from other purse seine fishing companies operating in the Atlantic and Indian Oceans since the French purse seine fleet only represented about 20% of the total purse seine catch in recent years. Recent availability of FAD GPS positions in the western and central Pacific Ocean shows a positive step in this direction (Escalle et al., 2017). It would also be beneficial to apply the GDP's quality control procedures (Hansen and Poulain, 1996; Lumpkin and Pazos, 2007) to the FAD data. This step may provide useful information that is currently missing such as FAD location errors.

More broadly, the conspicuous character of global changes presents some serious observational challenges. Effectively responding to these challenges requires better integration across individual networks and multiple platforms, to make the most of synergies between the different types of ocean observations (Roemmich et al., 2010). The development of standards for metadata and data formats, as well as access protocols (e.g., Web Services), has recently enhanced interoperability functions in information systems. Thus, these standards are better able to merge and process heterogeneous data sets stored in distributed infrastructures and promote integration across scientific disciplines (Reichman et al., 2011; Mooney et al., 2013; Robertson et al., 2014). Data management systems should also include well-described control procedures that aim to inform users about the best quality data sets available (Roemmich et al., 2010). In oceanography, the recent introduction of key standards contributes to this higher level of interoperability for physical and chemical parameters delivered as gridded data (e.g. model outputs, or satellite remote-sensing products) or time series of parameters retrieved from platforms at sea (Hankin et al., 2010). Like the data collected through citizen science initiatives (Lauro et al., 2014), the millions of data collected by fishermen could substantially increase the spatio-temporal coverage of ocean observations in a cost-efficient manner. Thus, the major contributions these data sets could potentially make to the GOOS and GCOS calls for improved collaboration with the fishing industry and the establishment of a system that adequately acknowledges the contributors and fosters a data sharing environment.

Acknowledgements

We are grateful to ORTHONGEL and the fishing companies CFTO, SAPMER, and SAUPIQUET for making their FAD buoy data available and open access. We are particularly grateful to Laurent Pinault, Sarah Le Couls, Anthony Claude, Martin Denniel, Gildas Bodilis, David Kaplan and Laurent Floch for their assistance with the data management and interpretation. Many thanks to Iñigo Krug for sharing information on FAD design and Pierre Lopez for his assistance in preparing the artwork. We would also like to thank the AOML's drifting buoy group for making their drifter data available and acknowledge the OSCAR Project Office for providing the surface current data. Thanks to Pierrick Penven for pointing out some useful references, Daniel Gaertner for his statistical advice, and Joël Sudre, Thierry Delcroix, Eric Greiner, Nathalie Bodin, Rick Lumpkin and an anonymous reviewer for their useful comments on earlier versions of this study. This work received funding from France Filière Pêche (FFP) through the PhD. grant of AM (FFP PH/2012/14 and IRD 303291/00), the European project CECOFAD (MARE/2012/24), the European Union's Horizon 2020 research and innovation program under the BlueBRIDGE project (Grant agreement No 675680), and the Observatoire Thonier of IRD. We are grateful to Jane Alpine and Anne-Elise Nieblas for carefully editing the manuscript.

Appendix

Table A1: Total number of fish aggregating device (FAD) and drifter observations collected in the Longhurst biogeographical provinces between 2008 and 2014. Selected provinces are shaded.

Province description	Code	Drifters	FADs
Australia-Indonesia Coastal Province	AUSW	16,651	6,106
Benguela Current Coastal Province	BENG	6,431	1,858
Brazil Current Coastal Province	BRAZ	19,616	1,399
Canary Coastal Province	CNRY	13,085	21,399
China Sea Coastal Province	CHIN	4,126	0
E. Africa Coastal Province	EAFR	31,118	175,733
E. India Coastal Province	INDE	10,248	237
Guianas Coastal Province	GUIA	12,693	8,946
Guinea Current Coastal Province	GUIN	8,009	234,069
NW Arabian Upwelling Province	ARAB	23,400	367,690
Red Sea, Persian Gulf Province	REDS	39	10
Sunda-Arafura Shelves Province	SUND	6,872	83
SW Atlantic Shelves Province	FKLD	189	0
W. India Coastal Province	INDW	5,494	2,401
Archipelagic Deep Basins Province	ARCH	27,079	554
Caribbean Province	CARB	2,515	174
Eastern Tropical Atlantic Province	ETRA	59,360	780,874
Indian Monsoon Gyres Province	MONS	146,705	2,665,216
Indian S. Subtropical Gyre Province	ISSG	160,585	162,963
N. Atlantic Tropical Gyral Province	NATR	184,482	63,101
South Atlantic Gyral Province	SATL	260,199	47,029
Western Tropical Atlantic Province	WTRA	57,414	230,438
S. Subtropical Convergence Province	SSTC	34,404	805
Subantarctic Province	SANT	1,603	27
N. Atlantic Subtropical Gyral Province (East)	NASE	0	87

Table A2: The first quartile, median, and third quartile values (cm s^{-1}) from the fish aggregating device (FAD) and drifter velocity distributions in selected Longhurst biogeographical provinces of the Atlantic (upper part of the table) and Indian (lower part) Oceans (see Appendix Table A1 for acronyms of the provinces and Fig. 2 for their location).

Device	Province	1st quartile	Median	3rd quartile
Drifters	ETRA	11.62	19.65	31.45
FADs	ETRA	12.08	20.29	31.91
Drifters	GUIN	13.07	23.05	38.60
FADs	GUIN	8.91	15.98	28.49
Drifters	NATR	8.36	13.39	19.95
FADs	NATR	9.03	15.09	24.42
Drifters	WTRA	15.47	26.73	42.99
FADs	WTRA	15.58	27.39	44.18
Drifters	ARAB	14.22	23.79	39.19
FADs	ARAB	27.17	45.67	75.87
Drifters	EAFR	18.77	33.28	56.74
FADs	EAFR	22.63	36.72	55.12
Drifters	ISSG	13.70	22.20	33.39
FADs	ISSG	18.36	28.56	40.73
Drifters	MONS	17.00	27.89	43.64
FADs	MONS	21.27	34.51	52.65

Table A3: The number of observations, correlation coefficients and slope of the velocity components for fish aggregating devices (FADs) versus drifters at different spatio-temporal buffers in the Atlantic and Indian Oceans.

Ocean	deltaD_deg	deltaT_day	speed_component	n	Corr	Slope	Slope_lower	Slope_upper
Indian	1/6	0.5	velocity	10,015	0.85	1	1	1.01
Indian	1/6	1	velocity	14,556	0.83	1.01	1	1.01
Indian	1/6	2.5	velocity	25,956	0.78	1.02	1.02	1.03
Atlantic	1/6	0.5	velocity	2,842	0.73	1.12	1.1	1.14
Atlantic	1/6	1	velocity	4,146	0.75	1.15	1.13	1.16
Atlantic	1/6	2.5	velocity	7,739	0.71	1.2	1.18	1.21
Indian	1/6	0.5	u	10,015	0.93	1	0.99	1
Indian	1/6	1	u	14,556	0.93	1	0.99	1.01
Indian	1/6	2.5	u	25,956	0.9	1.01	1	1.01
Atlantic	1/6	0.5	u	2,842	0.87	1.16	1.14	1.19
Atlantic	1/6	1	u	4,146	0.87	1.17	1.15	1.19
Atlantic	1/6	2.5	u	7,739	0.85	1.21	1.19	1.22
Indian	1/6	0.5	v	10,015	0.88	1.02	1.01	1.03
Indian	1/6	1	v	14,556	0.85	1.04	1.03	1.05
Indian	1/6	2.5	v	25,956	0.77	1.08	1.07	1.09
Atlantic	1/6	0.5	v	2,842	0.69	1.06	1.02	1.1
Atlantic	1/6	1	v	4,146	0.68	1.16	1.12	1.2
Atlantic	1/6	2.5	v	7,739	0.58	1.33	1.29	1.37

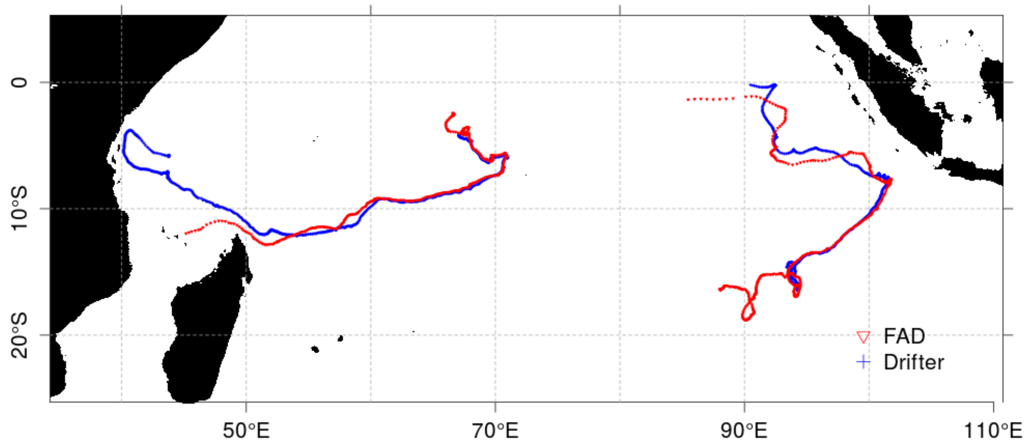

Figure A1: Examples of long-associated drift across the Indian Ocean featuring fish aggregating device (FAD) buoy n°17179 (red triangles) and drifter n°109550 (blue crosses) on the left, FAD buoy n°16812 and drifter n°109364 on the right, sharing similar trajectories between August and November 2013.

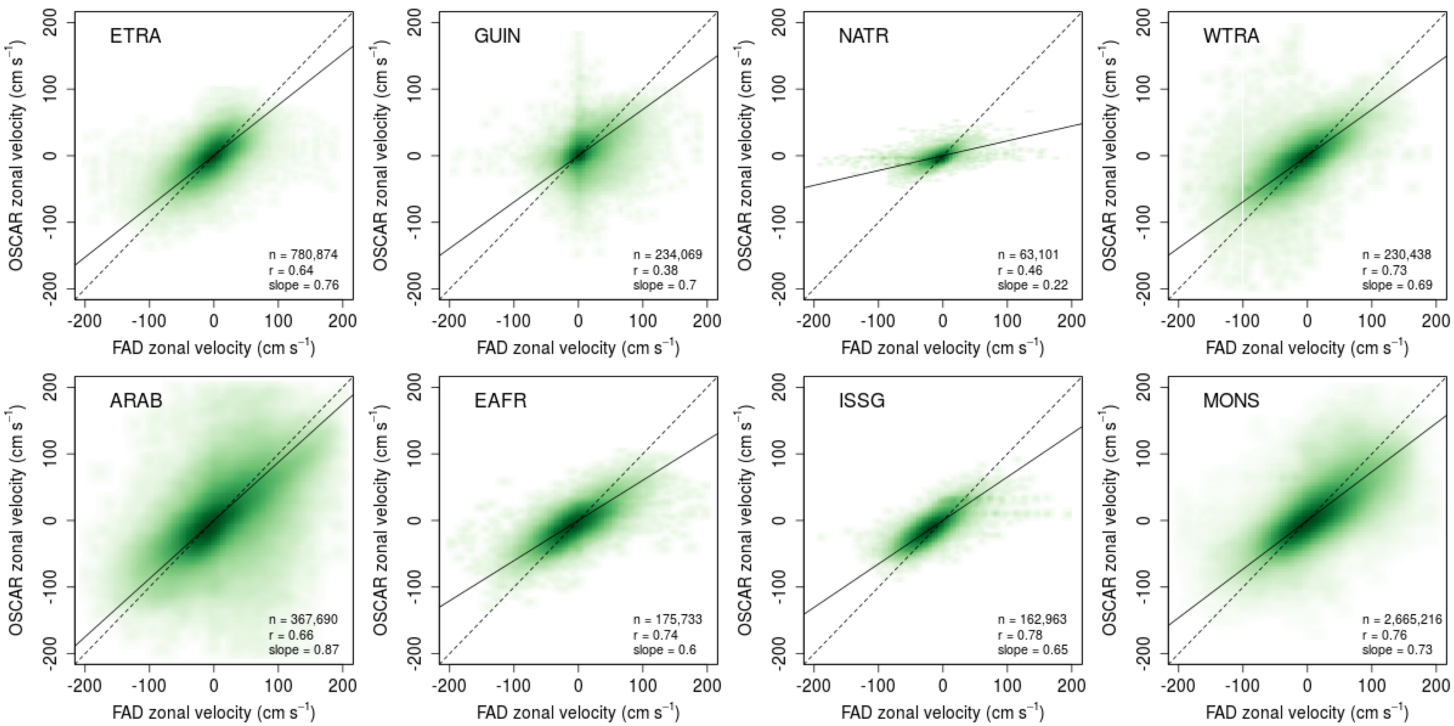

Figure A2: The comparison of zonal velocities between fish aggregating devices (FADs) and Ocean Surface Currents Analyses Real-time (OSCAR) in the selected Longhurst biogeographical provinces of the Atlantic Ocean (top) and Indian Ocean (bottom). The solid line indicates the major axis regression model and the dashed line indicates the 1:1 isoline.

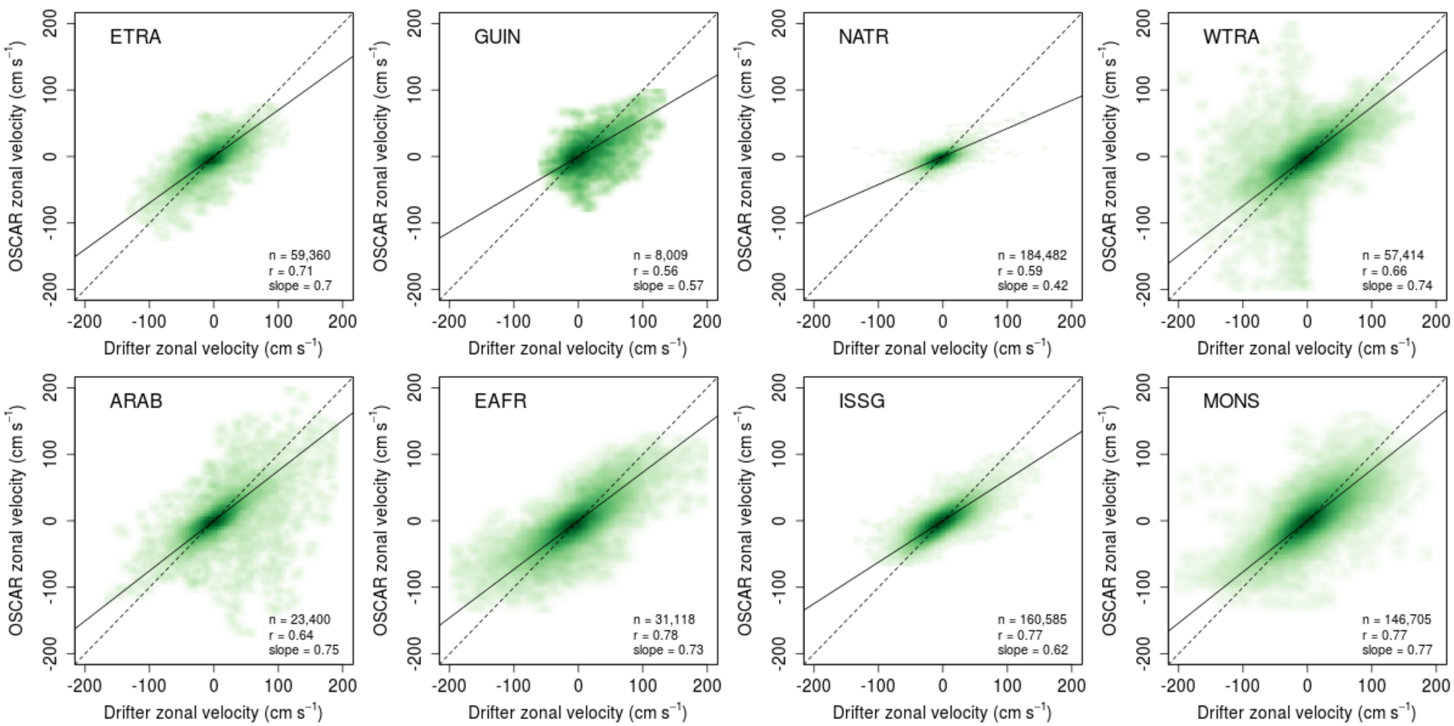

Figure A3: The comparison of zonal velocities between drifters and Ocean Surface Currents Analyses Real-time (OSCAR) in the selected Longhurst biogeographical provinces of the Atlantic Ocean (top) and Indian Ocean (bottom). The solid line indicates the major axis regression model and the dashed line indicates the 1:1 isoline.

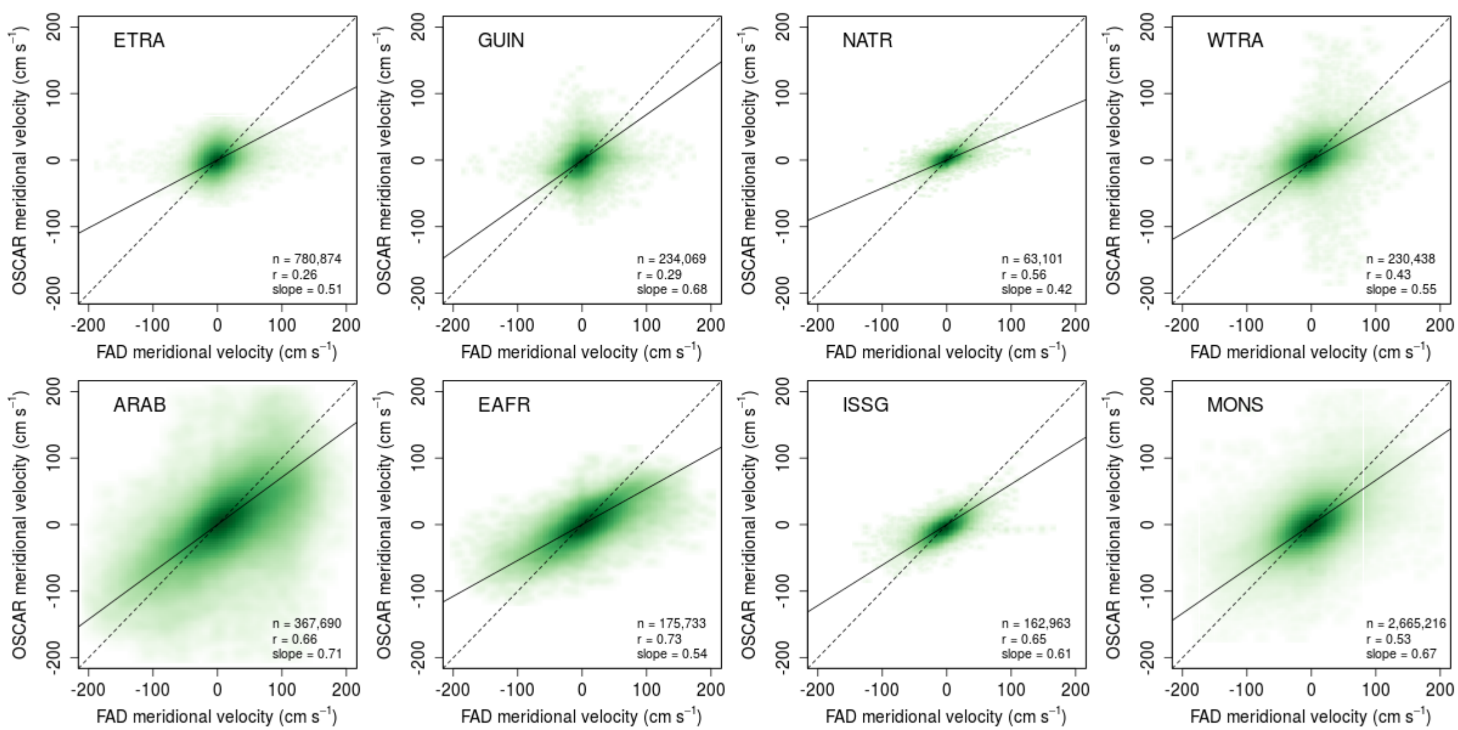

Figure A4: The comparison of meridional velocities between fish aggregating devices (FADs) and Ocean Surface Currents Analyses Real-time (OSCAR) in the selected Longhurst biogeographical provinces of the Atlantic Ocean (top) and Indian Ocean (bottom). The solid line indicates the major axis regression model and the dashed line indicates the 1:1 isoline.

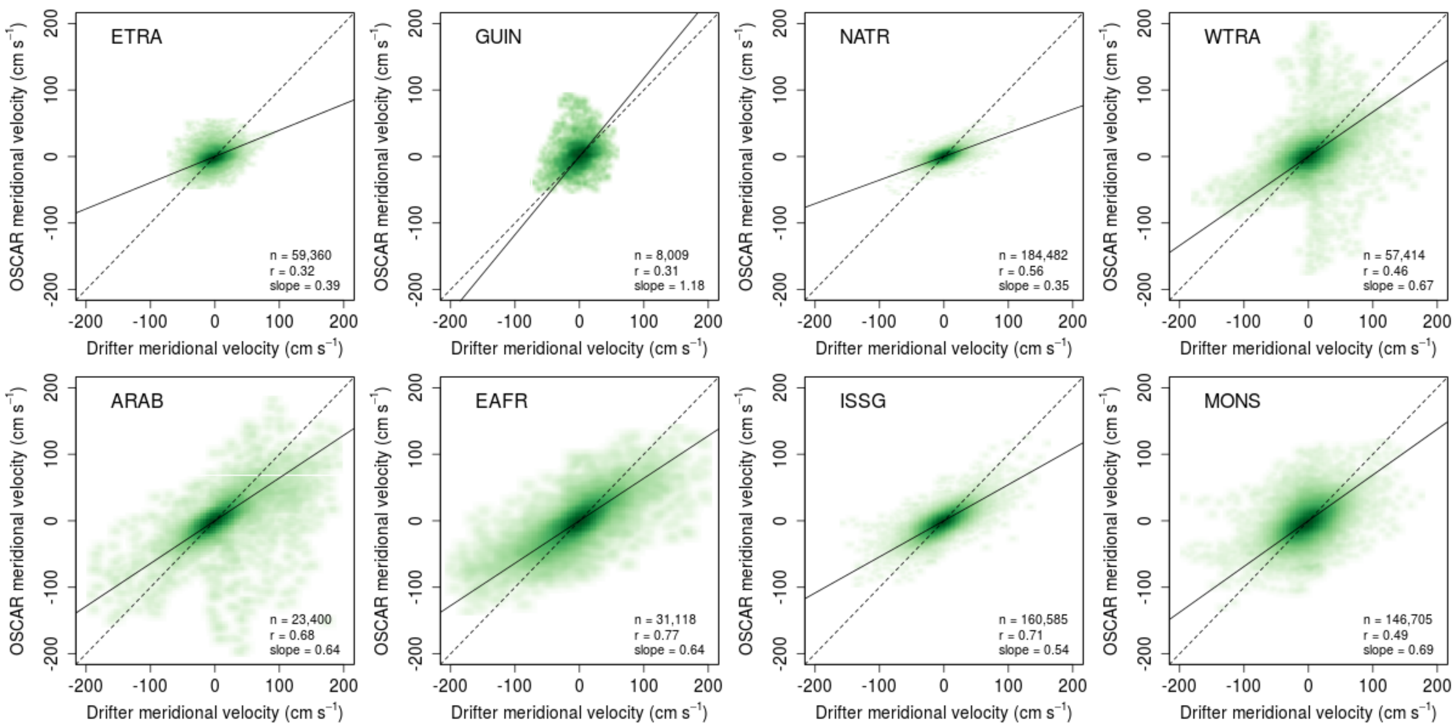

Figure A5: The comparison of meridional velocities between drifters and Ocean Surface Currents Analyses Real-time (OSCAR) in the selected Longhurst biogeographical provinces of the Atlantic Ocean (top) and Indian Ocean (bottom). The solid line indicates the major axis regression model and the dashed line indicates the 1:1 isoline.

Table A4: Summary of the major axis regression models fitted to the velocity components of the Ocean Surface Currents Analyses Real-time (OSCAR) measurements versus fish aggregating devices (FADs) and OSCAR versus drifters in the selected Longhurst biogeographical provinces of the Atlantic and Indian Oceans. Slope low. = 2.5% quantile value used as the lower limit of the regression slope estimate; Slope upp. = 97.5% quantile value used as the upper limit of the regression slope estimate. r = Pearson's correlation coefficient.

Device	Component	Province	Slope low.	Slope	Sloper upp.	r
FADs	Zonal	ETRA	0.760	0.762	0.764	0.64
FADs	Zonal	GUIN	0.689	0.695	0.702	0.38
FADs	Zonal	NATR	0.220	0.223	0.225	0.46
FADs	Zonal	WTRA	0.690	0.693	0.695	0.73
FADs	Zonal	ARAB	0.870	0.874	0.877	0.66
FADs	Zonal	EAFR	0.601	0.603	0.606	0.74
FADs	Zonal	ISSG	0.651	0.652	0.654	0.78
FADs	Zonal	MONS	0.730	0.731	0.731	0.76
Drifters	Zonal	ETRA	0.692	0.698	0.703	0.71
Drifters	Zonal	GUIN	0.550	0.568	0.587	0.56
Drifters	Zonal	NATR	0.419	0.422	0.424	0.59
Drifters	Zonal	WTRA	0.737	0.744	0.750	0.66
Drifters	Zonal	ARAB	0.741	0.753	0.764	0.64
Drifters	Zonal	EAFR	0.723	0.729	0.735	0.78
Drifters	Zonal	ISSG	0.620	0.623	0.625	0.77
Drifters	Zonal	MONS	0.766	0.769	0.773	0.77
FADs	Meridional	ETRA	0.506	0.510	0.514	0.26
FADs	Meridional	GUIN	0.674	0.684	0.693	0.29
FADs	Meridional	NATR	0.415	0.420	0.425	0.56
FADs	Meridional	WTRA	0.548	0.553	0.557	0.43
FADs	Meridional	ARAB	0.709	0.711	0.714	0.66
FADs	Meridional	EAFR	0.536	0.538	0.541	0.73
FADs	Meridional	ISSG	0.605	0.608	0.611	0.65
FADs	Meridional	MONS	0.665	0.666	0.668	0.53
Drifters	Meridional	ETRA	0.385	0.394	0.403	0.32
Drifters	Meridional	GUIN	1.094	1.175	1.264	0.31
Drifters	Meridional	NATR	0.352	0.355	0.357	0.56
Drifters	Meridional	WTRA	0.659	0.670	0.680	0.46
Drifters	Meridional	ARAB	0.634	0.643	0.652	0.68
Drifters	Meridional	EAFR	0.632	0.638	0.644	0.77
Drifters	Meridional	ISSG	0.540	0.543	0.545	0.71
Drifters	Meridional	MONS	0.682	0.688	0.694	0.49

Table A5: The number of observations and correlation coefficients of the velocity components of Ocean Surface Currents Analyses Real-time (OSCAR) versus fish aggregating devices (FADs) and OSCAR versus drifters for the entire dataset (n, Corr_u, Corr_v) and for the datasets subsampled every 5 days (n5, corr5_u, corr5_v) and 15 days (n15, corr15_u, corr15_v) in the Atlantic and Indian Oceans.

X	Device	Ocean	n	Corr_u	Corr_v	n5	corr5_u	corr5_v	n15	corr15_u	corr15
1	FADs	Atlantic	1,393,100	0.62	0.31	66,228	0.57	0.27	36,986	0.53	0.24
2	FADs	Indian	3,384,424	0.75	0.58	181,193	0.72	0.56	108,611	0.70	0.55
3	Drifters	Atlantic	634,297	0.58	0.49	32,303	0.58	0.47	11,211	0.57	0.49
4	Drifters	Indian	458,065	0.74	0.63	23,418	0.75	0.64	8,187	0.77	0.65

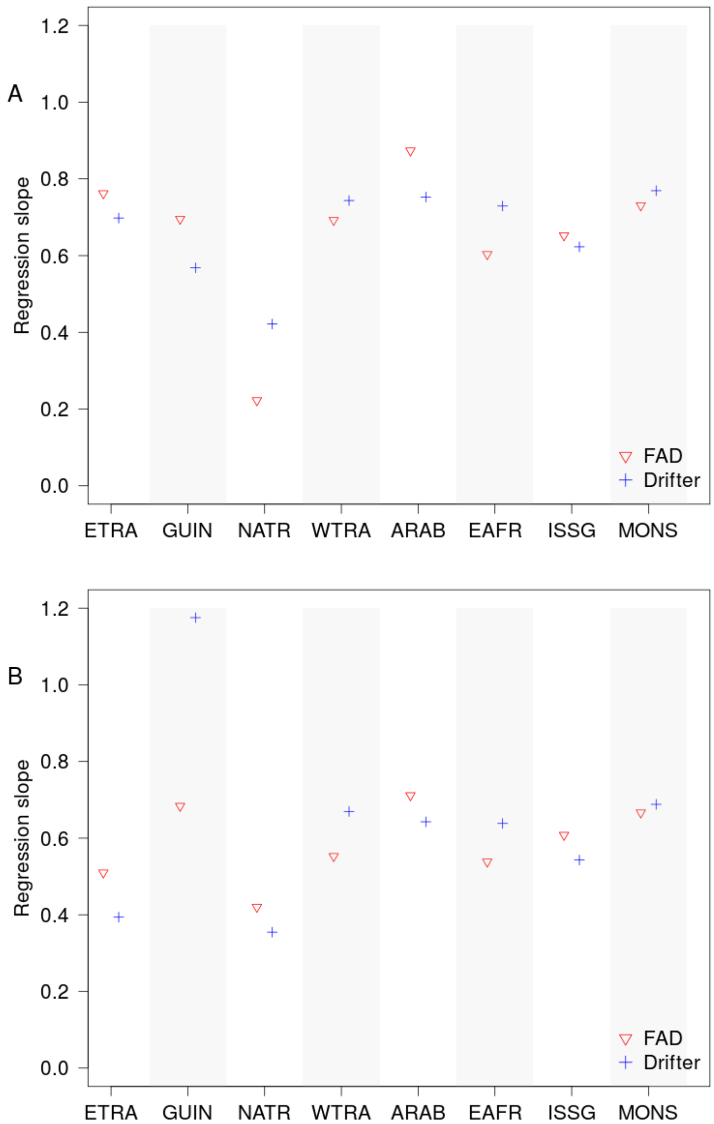

Figure A6: The comparison of slopes of major axis regression models fitted to the (A) zonal and (B) meridional velocity data of the Ocean Surface Currents Analyses Real-time (OSCAR) versus fish aggregating devices (FADs) and OSCAR versus drifters in the selected Longhurst biogeographical provinces.

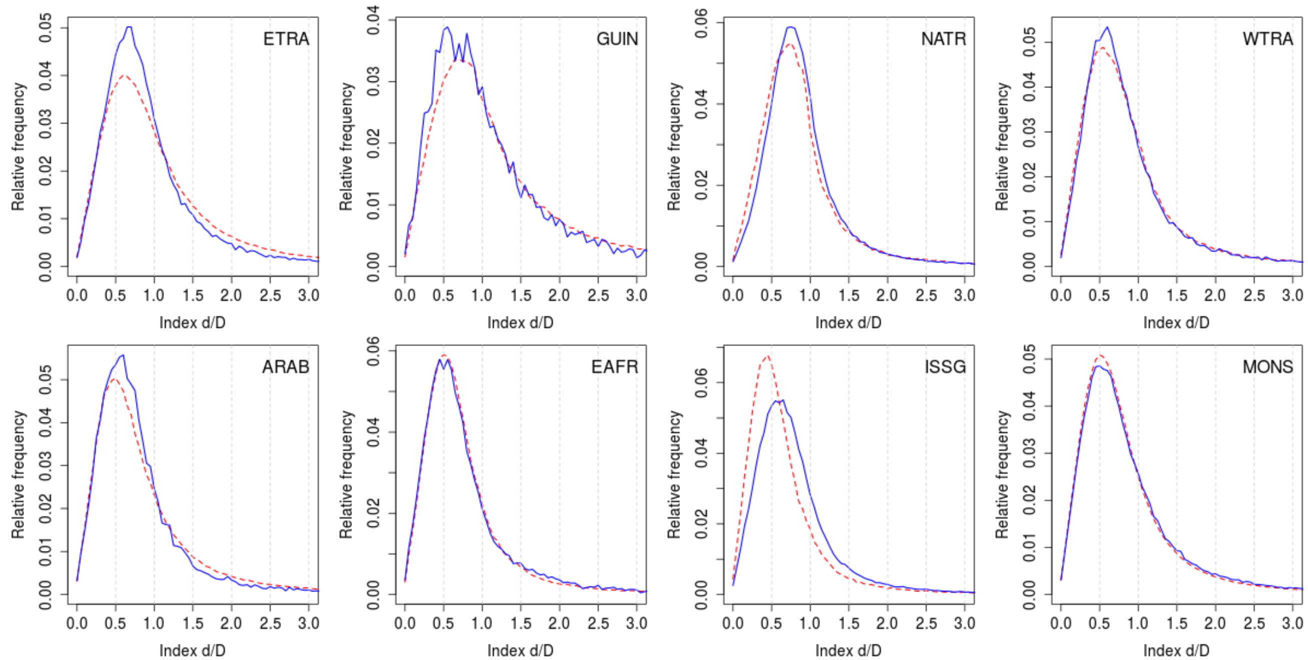

Figure A7: Relative frequency distributions of the index d/D that describe the prediction skill of fish aggregating devices (FADs; dashed red curves) and drifters (solid blue curves), with respect to the Ocean Surface Currents Analyses Real-time (OSCAR) velocities for the selected Longhurst biogeographical provinces, where d is the distance between the projected and observed location at the next time step and D is the distance between the current and next observed locations.

References

A. Baske, J. Gibbon, J. Benn, and A. Nickson. Estimating the use of drifting Fish Aggregation Devices (FADs) around the globe. Discussion Paper, PEW Environment Group, 2012.

Maristella Berta, Lucio Bellomo, Marcello G. Magaldi, Annalisa Griffa, Anne Molcard, Julien Marmain, Mireno Borghini, and Vincent Taillandier. Estimating Lagrangian transport blending drifters with HF radar data and models: Results from the TOSCA experiment in the Ligurian Current (North Western Mediterranean Sea). Progress in Oceanography, 128: 15–29, November 2014. ISSN 0079-6611. doi: 10.1016/j.pocean.2014.08.004. URL `http://www.sciencedirect.com/science/article/pii/S007966111400127X`.

Emmanuel Chassot, S. Bonhommeau, G. Reygondeau, K. Nieto, J. J Polovina, M. Huret, N. K Dulvy, and Hervé Demarcq. Satellite remote sensing for an ecosystem approach to fisheries management. ICES Journal of Marine Science, 68:651–666, 2011. ISSN 1054-3139. doi: 10.1093/icesjms/fsq195. URL `http://www.documentation.ird.fr/hor/fdi:010053407`.

Andrés Cózar, Fidel Echevarría, J. Ignacio González-Gordillo, Xabier Irigoien, Bárbara Úbeda, Santiago Hernández-León, Álvaro T. Palma, Sandra Navarro, Juan García-de Lomas, Andrea Ruiz, María L. Fernández-de Puelles, and Carlos M. Duarte. Plastic debris in the open ocean. Proceedings of the National Academy of Sciences, 111(28):10239–10244, July 2014. ISSN 0027-8424, 1091-6490. doi: 10.1073/pnas.1314705111. URL `http://www.pnas.org/content/111/28/10239`.

Fraser Davidson, Arthur Allen, Gary Brassington, Øyvind Breivik, Pierre Daniel, Masafumi Kamachi, Satoshi Sato, Brian King, Fabien Lefevre, and Marion Sutton. Applications of GODAE ocean current forecasts to search and rescue and ship routing. Oceanography, 22(3):176–181, September 2009. ISSN 10428275. doi: 10.5670/oceanog.2009.76. URL `http://dx.doi.org/10.5670/oceanog.2009.76`.

Kathleen Dohan and Nikolai Maximenko. Monitoring ocean currents with satellite sensors. Oceanography, 23(4):94–103, December 2010. ISSN 10428275. doi: 10.5670/oceanog.2010.08. URL `http://dx.doi.org/10.5670/oceanog.2010.08`.

Marie Drévillon, Eric Greiner, Denis Paradis, Christophe Payan, Jean-Michel Lellouche, Guillaume Reffray, Edmée Durand, Stéphane Law-Chune, and Sylvain Cailleau. A strategy for producing refined currents in the Equatorial Atlantic in the context of the search of the AF447 wreckage. Ocean Dynamics, 63(1):63–82, January 2013. ISSN 1616-7341, 1616-7228. doi: 10.1007/s10236-012-0580-2. URL http://link.springer.com/10.1007/s10236-012-0580-2.

Shane Elipot, Rick Lumpkin, Renellys C. Perez, Jonathan M. Lilly, Jeffrey J. Early, and Adam M. Sykulski. A global surface drifter data set at hourly resolution. Journal of Geophysical Research: Oceans, 121 (5):2937–2966, 2016. URL http://onlinelibrary.wiley.com/doi/10.1002/2016JC011716/full.

L. Escalle, S. Brouwer, J. Scutt Philipps, G. Pilling, and PNA office. Preliminary analysis of PNA FAD tracking data from 2016 and 2017. volume WCPFC-SC13-2017/MI-WP-05, page 21p, Rarotonga, Cook Islands, 2017. WCPFC.

Alain Fonteneau, Emmanuel Chassot, and Nathalie Bodin. Global spatio-temporal patterns in tropical tuna purse seine fisheries on drifting fish aggregating devices (DFADs): Taking a historical perspective to inform current challenges. Aquatic Living Resources, 26(1):37–48, April 2013. ISSN 0990-7440, 1765-2952. doi: 10.1051/alr/2013046. URL http://www.alr-journal.org/10.1051/alr/2013046.

J. Franco, L. Dagorn, I. Sancristobal, and G. Moreno. Design of ecological FADs. volume IOTC-2009-WPEB-16, page 22, Mombasa, Kenya, 12-14 October 2009, 2009. IOTC.

Eric Freeman, Scott D. Woodruff, Steven J. Worley, Sandra J. Lubker, Elizabeth C. Kent, William E. Angel, David I. Berry, Philip Brohan, Ryan Eastman, Lydia Gates, Wolfgang Gloeden, Zaihua Ji, Jay Lawrimore, Nick A. Rayner, Gudrun Rosenhagen, and Shawn R. Smith. ICOADS Release 3.0: a major update to the historical marine climate record. International Journal of Climatology, 37(5):2211–2232, 2017. ISSN 1097-0088. doi: 10.1002/joc.4775. URL http://onlinelibrary.wiley.com/doi/10.1002/joc.4775/abstract.

Pierre Fréon and Laurent Dagorn. Review of fish associative behaviour: Toward a generalisation of the meeting point hypothesis. *Reviews in Fish Biology and Fisheries*, 10(2):183–207, 2000. ISSN 0960-3166. doi: 10.1023/A:1016666108540. URL http://dx.doi.org/10.1023/A:1016666108540.

C. Gnanaseelan and Aditi Deshpande. Equatorial indian ocean subsurface current variability in an ocean general circulation model. *Climate Dynamics*, pages 1–13, May 2017. ISSN 0930-7575, 1432-0894. doi: 10.1007/s00382-017-3716-8. URL http://dx.doi.org/10.1007/s00382-017-3716-8.

M. Hall and M.H. Roman. The fishery on fish-aggregating devices (FADs) in the Eastern Pacific Ocean - Update. volume SAC-08-03e, page 19p, La Jolla, California, U.S.A., 2017. IATTC.

Steve C. Hankin, Jon D. Blower, Thierry Carval, Kenneth S. Casey, Craig Donlon, Olivier Lauret, Thomas Loubrieu, Ashwanth Srinivasan, Joaquin Trinanes, Oystein Godoy, Roy Mendelssohn, Rich Signell, Jeff de la Beaujardiere, Peter Cornillon, Frédérique Blanc, Russ Rew, and Jack Harlan. NetCDF-CF-OPeNDAP: Standards for ocean data interoperability and object lessons for community data standards processes. In *Proceedings of OceanObs'09: Sustained Ocean Observations and Information for Society*, volume 2, 21-25 septembre 2009, Venice, Italy, 2010. Hall, J., Harrison, D.E. & Stammer, D. doi: 10.5270/OceanObs09.cwp.41. URL http://archimer.ifremer.fr/doc/00027/13832/10969.pdf.

Donald V. Hansen and Pierre-Marie Poulain. Quality control and interpolations of WOCE-TOGA drifter data. *Journal of Atmospheric and Oceanic Technology*, 13(4):900–909, August 1996. ISSN 0739-0572. doi: 10.1175/1520-0426(1996)013⟨0900:QCAIOW⟩2.0.CO;2. URL http://journals.ametsoc.org/doi/abs/10.1175/1520-0426(1996)013%3C0900%3AQCAIOW%3E2.0.CO%3B2.

W. E. Johns, P. Brandt, B. Bourlès, A. Tantet, A. Papapostolou, and A. Houk. Zonal structure and seasonal variability of the Atlantic Equatorial Undercurrent. *Climate Dynamics*, 43(11):3047–3069, December 2014. ISSN 0930-7575, 1432-0894. doi: 10.1007/s00382-014-2136-2. URL http://dx.doi.org/10.1007/s00382-014-2136-2.

Eric S. Johnson, Fabrice Bonjean, Gary S. E. Lagerloef, John T. Gunn, and Gary T. Mitchum. Validation and error analysis of OSCAR sea surface currents. Journal of Atmospheric and Oceanic Technology, 24(4):688–701, 2007. ISSN 0739-0572. doi: 10.1175/JTECH1971.1. URL http://dx.doi.org/10.1175/JTECH1971.1.

Antony Joseph. Measuring Ocean Currents: Tools, Technologies, and Data. Newnes, August 2013. ISBN 978-0-12-391428-6.

E.C. Kent, G. Ball, D.I. Berry, J. Fletcher, A. Hall, S. North, and S. D. Woodruff. The Voluntary Observer Ship (VOS) scheme. In Proceedings of OceanObs'09, volume 2 of ESA Special Publication, WPP-306, pages 551–561, Venice, Italy, 21-25 September 2009, 2010. Hall, J., Harrison, D.E. & Stammer, D.

Gary S. E. Lagerloef, Gary T. Mitchum, Roger B. Lukas, and Pearn P. Niiler. Tropical Pacific near-surface currents estimated from altimeter, wind, and drifter data. Journal of Geophysical Research: Oceans, 104(C10): 23313–23326, October 1999. ISSN 2156-2202. doi: 10.1029/1999JC900197. URL http://onlinelibrary.wiley.com/doi/10.1029/1999JC900197/abstract.

Federico M. Lauro, Svend Jacob Senstius, Jay Cullen, Russell Neches, Rachelle M. Jensen, Mark V. Brown, Aaron E. Darling, Michael Givskov, Diane McDougald, Ron Hoeke, Martin Ostrowski, Gayle K. Philip, Ian T. Paulsen, and Joseph J. Grzymski. The common oceanographer: Crowdsourcing the collection of oceanographic data. PLOS Biology, 12(9): e1001947, September 2014. ISSN 1545-7885. doi: 10.1371/journal.pbio.1001947. URL http://journals.plos.org/plosbiology/article?id=10.1371/journal.pbio.1001947.

Kara Lavender Law, Skye Morét-Ferguson, Nikolai A. Maximenko, Giora Proskurowski, Emily E. Peacock, Jan Hafner, and Christopher M. Reddy. Plastic accumulation in the North Atlantic subtropical gyre. Science, 329 (5996):1185–1188, September 2010. ISSN 0036-8075, 1095-9203. doi: 10.1126/science.1192321. URL http://science.sciencemag.org/content/329/5996/1185.

Tong Lee, Sirpa Hakkinen, Kathie Kelly, Bo Qiu, Hans Bonekamp, and Eric J. Lindstrom. Satellite observations of ocean circulation changes associated with climate variability. Oceanography, 23(4):70, 2010. URL http://www.jstor.org/stable/24860863.

P. Legendre and L. Legendre. Numerical ecology. Elsevier Science, New York, USA, 1998.

A. R Longhurst. Ecological geography of the sea. Academic Press, London, UK, 2007.

Rick Lumpkin and S. Elipot. Surface driter pair spreading in the North Atlantic. Journal of Geophysical Research, 115:C12017, 2010. doi: 10.1029/2010JC006338.

Rick Lumpkin and Gregory C. Johnson. Global ocean surface velocities from drifters: Mean, variance, El Niño–Southern Oscillation response, and seasonal cycle. Journal of Geophysical Research: Oceans, 118(6):2992–3006, 2013. ISSN 2169-9291. doi: 10.1002/jgrc.20210. URL http://dx.doi.org/10.1002/jgrc.20210.

Rick Lumpkin and Mayra Pazos. Measuring surface currents with Surface Velocity Program drifters: the instrument, its data, and some recent results. In Lagrangian analysis and prediction of coastal and ocean dynamics, pages 39–67. Cambridge University Press, griffa a, kirwan a.d., mariano a.j., Özgökmen t, rossby t edition, 2007. URL https://books.google.com/books?hl=en&lr=&id=UgUdrv_RWmkC&oi=fnd&pg=PA39&dq=lumpkin+global+drifter+program&ots=93P8A2SomL&sig=hweik3Vsk2hBERGOrUrkHn7aNiI.

M. Manyilizu, P. Penven, and C. J. C. Reason. Annual cycle of the upper-ocean circulation and properties in the tropical western indian ocean. African Journal of Marine Science, 38(1):81–99, April 2016. ISSN 1814-232X. doi: 10.2989/1814232X.2016.1158123. URL http://dx.doi.org/10.2989/1814232X.2016.1158123.

S. Martin. An introduction to ocean remote sensing. Cambridge University Press, June 2004. ISBN 978-0-521-80280-2.

Alexandra Maufroy, Emmanuel Chassot, Rocío Joo, and David Michael Kaplan. Large-scale examination of spatio-temporal patterns of drifting fish aggregating devices (dFADs) from tropical tuna fisheries of the Indian and Atlantic oceans. PLoS ONE, 10(5):e0128023, 2015. doi: 10.1371/journal.pone.0128023. URL http://dx.doi.org/10.1371/journal.pone.0128023.

Alexandra Maufroy, David M. Kaplan, Nicolas Bez, De Molina, Alicia Delgado, Hilario Murua, Laurent Floch, and Emmanuel Chassot. Massive increase in the use of drifting Fish Aggregating Devices (dFADs) by tropical tuna purse seine fisheries in the Atlantic and Indian oceans. ICES Journal of Marine Science, 74(1):215–225, January 2017. ISSN 1054-3139. doi: 10.1093/icesjms/fsw175. URL https://academic.oup.com/icesjms/article-abstract/74/1/215/2418180/Massive-increase-in-the-use-of-drifting-Fish.

Nikolai Maximenko, Peter Niiler, Luca Centurioni, Marie-Helene Rio, Oleg Melnichenko, Don Chambers, Victor Zlotnicki, and Boris Galperin. Mean Dynamic Topography of the Ocean Derived from Satellite and Drifting Buoy Data Using Three Different Techniques. Journal of Atmospheric and Oceanic Technology, 26(9):1910–1919, September 2009. ISSN 0739-0572. doi: 10.1175/2009JTECHO672.1. URL http://journals.ametsoc.org/doi/abs/10.1175/2009jtecho672.1.

H. A. Mooney, A. Duraiappah, and A. Larigauderie. Evolution of natural and social science interactions in global change research programs. Proceedings of the National Academy of Sciences of the United States of America, 110: 3665–3672, 2013.

J. Murua, G. Moreno, D. Itano, M. Hall, L. Dagorn, and V. Restrepo. ISSF Skippers' Workshops Round 7. ISSF Technical Report 2018-01, ISSF, Washington D.C., U.S.A., 2018.

Pearn P. Niiler and Jeffrey D. Paduan. Wind-Driven Motions in the Northeast Pacific as Measured by Lagrangian Drifters. Journal of Physical Oceanography, 25(11):2819–2830, November 1995. ISSN 0022-3670, 1520-0485. doi: 10.1175/1520-0485(1995)025⟨2819:WDMITN⟩2.0.CO;2. URL http://journals.ametsoc.org/doi/abs/10.1175/1520-0485%281995%29025%3C2819%3AWDMITN%3E2.0.CO%3B2.

Shiqiu Peng, Yu-Kun Qian, Rick Lumpkin, Yan Du, Dongxiao Wang, and Ping Li. Characteristics of the near-surface currents in the Indian Ocean as deduced from satellite-tracked surface drifters. part i: pseudo-Eulerian statistics. Journal of Physical Oceanography, 45(2):441–458, November 2014. ISSN 0022-3670. doi: 10.1175/JPO-D-14-0050.1. URL http://journals.ametsoc.org/doi/abs/10.1175/JPO-D-14-0050.1.

Pierre-Marie Poulain, Riccardo Gerin, Elena Mauri, and Romain Pennel. Wind effects on drogued and undrogued drifters in the eastern mediterranean. Journal of Atmospheric and Oceanic Technology, 26(6):1144–1156, June 2009. ISSN 0739-0572. doi: 10.1175/2008JTECHO618.1. URL http://dx.doi.org/10.1175/2008JTECHO618.1.

O.J. Reichman, M.B. Jones, and M.P. Schildhauer. Challenges and opportunities of open data in ecology. Science, 331:703–705, 2011.

Gilles Reverdin, P. P. Niiler, and H. Valdimarsson. North Atlantic Ocean surface currents. Journal of Geophysical Research: Oceans, 108(C1):3002, January 2003. ISSN 2156-2202. doi: 10.1029/2001JC001020. URL http://onlinelibrary.wiley.com/doi/10.1029/2001JC001020/abstract.

R.W. Reynolds and N.A. Rayner. An improved in situ and satellite SST analysis for climate. Journal of Climate, 15:1609–1625, 2002.

A. J Richardson and E. S Poloczanska. Under-resourced, under threat. Science, 320(5881):1294, 2008.

Tim Robertson, Markus Döring, Robert Guralnick, David Bloom, John Wieczorek, Kyle Braak, Javier Otegui, Laura Russell, and Peter Desmet. The GBIF Integrated Publishing Toolkit: Facilitating the efficient publishing of biodiversity data on the internet. PLOS ONE, 9(8): e102623, August 2014. ISSN 1932-6203. doi: 10.1371/journal.pone.0102623. URL http://journals.plos.org/plosone/article?id=10.1371/journal.pone.0102623.

D. Roemmich, L. Boehme, H. Claustre, H. Freeland, M. Fukasawa, G. Goni, W.G. Gould, N. Gruber, M. Hood, E. Kent, Rick Lumpkin, S. Smith, and P. Testor. Integrating the ocean observing system: Mobile platforms. In Proceedings of OceanObs'09: Sustained Ocean Observations and Information for Society, volume 1, pages 377–394, Venice, Italy, 21-25 September 2009, 2010. Hall, J., Harrison, D.E. & Stammer, D. doi: 10.5270/OceanObs09.pp.33.

G. Scott and J. Lopez. The use of FADs in tuna fisheries. Directorate-General for internal policies IP/B/PECH/IC/2013-123, European Union, 2014.

J. J Simpson. Remote sensing and geographical information systems: Their past, present and future use in global marine fisheries. Fisheries Oceanography, 1(3):238–280, 1992.

Joel Sudre and Rosemary A. Morrow. Global surface currents: a high-resolution product for investigating ocean dynamics. Ocean Dynamics, 58(2):101, May 2008. ISSN 1616-7341, 1616-7228. doi: 10.1007/s10236-008-0134-9. URL http://link.springer.com/article/10.1007/s10236-008-0134-9.

Edgar Torres-Irineo, Daniel Gaertner, Emmanuel Chassot, and Michel Dreyfus-León. Changes in fishing power and fishing strategies driven by new technologies: The case of tropical tuna purse seiners in the eastern Atlantic Ocean. Fisheries Research, 155:10–19, 2014. ISSN 0165-7836. doi: 10.1016/j.fishres.2014.02.017. URL http://www.sciencedirect.com/science/article/pii/S0165783614000575.

David I. Warton, Ian J. Wright, Daniel S. Falster, and Mark Westoby. Bivariate line-fitting methods for allometry. Biological Reviews, 81(2):259–291, May 2006. ISSN 1469-185X. doi: 10.1017/S1464793106007007. URL http://onlinelibrary.wiley.com/doi/10.1017/S1464793106007007/abstract.

Scott D. Woodruff, Ralph J. Slutz, Roy L. Jenne, and Peter M. Steurer. A Comprehensive Ocean-Atmosphere Data Set. Bulletin of the American Meteorological Society, 68(10):1239–1250, October 1987. ISSN 0003-0007. doi: 10.1175/1520-0477(1987)068⟨1239:ACOADS⟩2.0.CO;2. URL http://journals.ametsoc.org/doi/abs/10.1175/1520-0477(1987)068%3C1239:ACOADS%3E2.0.CO;2.

Max Yaremchuk, Peter Spence, Mozheng Wei, and Gregg Jacobs. Lagrangian predictability in the DWH region from HF radar observations and model output. Deep Sea Research Part II: Topical Studies in Oceanography, 129:394–400, July 2016. ISSN 0967-0645. doi: 10.1016/j.dsr2.2013.05.035. URL http://dx.doi.org/10.1016/j.dsr2.2013.05.035.